Hurricane Simulation and Nonstationary Extremal Analysis for a Changing Climate

MEAGAN CARNEY, A HOLGER KANTZ, AND MATTHEW NICOL

^a University of Queensland, Brisbane, Australia
^b Max Planck Institute for the Physics of Complex Systems, Dresden, Germany
^c University of Houston, Houston, Texas

(Manuscript received 28 November 2021, in final form 19 June 2022)

ABSTRACT: Particularly important to hurricane risk assessment for coastal regions is finding accurate approximations of return probabilities of maximum wind speeds. Since extremes in maximum wind speed have a direct relationship with minima in the central pressure, accurate wind speed return estimates rely heavily on proper modeling of the central pressure minima. Using the HURDAT2 database, we show that the central pressure minima of hurricane events can be appropriately modeled by a nonstationary extreme value distribution. We also provide and validate a Poisson distribution with a nonstationary rate parameter to model returns of hurricane events. Using our nonstationary models and numerical simulation techniques from established literature, we perform a simulation study to model returns of maximum wind speeds of hurricane events along the North Atlantic coast. We show that our revised model agrees with current data and results in an expectation of higher maximum wind speeds for all regions along the coast, with the highest maximum wind speeds occurring along the northeast seaboard.

KEYWORDS: Extreme events; Climate change; Hurricanes/typhoons; Numerical weather prediction/forecasting

1. Introduction

Hurricanes and tropical storms bring massive societal impacts and cause economic instabilities. Known for their high wind speeds and downpours, these storms are often accompanied by flooding, wind damage, and travel hazards that lead to large-scale evacuations and a national emergency response. Talk of climate change in recent years and more frequent observations of extreme weather events has inspired research into techniques that provide more accurate estimates of returns and return times of extremes (Bloemendaal et al. 2020; Carney et al. 2019; Carney and Kantz 2020; Knutson et al. 2019; Keim et al. 2004; Muller and Takayabu 2020; Patricola and Wehner 2018; Lucarini et al. 2016; Trepanier 2020).

Particularly important in hurricane risk assessment for coastal regions is finding accurate approximations of the return probabilities of maximum wind speeds. There have been several studies surrounding maximum wind speed return estimates for hurricanes occurring along the North Atlantic coast (Batts et al. 1980; Ho et al. 1987; Casson and Coles 2000; Simiu et al. 1995; Vickery and Twisdale 1995). Many of these studies use the retired HURDAT database, which has since been discounted as an unreliable source for future prediction modeling. Casson and Coles (2000) purposed a hurricane model that allows for approximations of maximum wind speed returns using the tracks and central pressure minima. The advantage of a model over raw data analysis is that a large number of hurricanes can be simulated to provide more accurate estimates of the tail probabilities and longer year returns of such rare events. The simulation results of this model are in good agreement with the other models and analyses of that decade. However, our findings suggest that this model does not hold up in accuracy when fitted to the updated

Corresponding author: Meagan Carney, m.carney@uq.edu.au

HURDAT2 database. These inaccuracies can be almost entirely attributed to systematic trends in the observed central pressure and frequency of hurricane events over recent years.

Although there are many factors in a hurricane event that affect the maximum wind speed, we find that the most influential for risk assessment are the central pressure minima and translational velocity of a hurricane at the time of impact with the coast. Since the central pressure minima have a direct relationship with the wind speed maxima, a better estimate of their probability distribution can provide more accurate returns of extreme highs of wind speed maxima along the coast. Models of an extreme (e.g., minima or maxima) most often take the form of an extreme value distribution (Coles 2001; Lucarini et al. 2016). These distributions have been studied extensively; however, revisions for more complex data analysis settings are often required.

Following the work in Casson and Coles (2000), we show that we can still reliably model the central pressure minima of a hurricane event using the generalized extreme value distribution (GEV); however, a previously unobserved time dependent trend in the central pressure minima requires adaptations in both the model and method. We also provide evidence for a Poisson distribution with a time-dependent rate parameter to model the number of yearly hurricane events that continues into the modern era (post-1965), which previous literature has assumed to be stationary (Casson and Coles 2000).

Recent work by Bloemendaal et al. (2020) has introduced a synthetic resampling algorithm (STORM) that can be applied to large-scale tropical cyclone datasets to extend the dataset in a way that preserves the statistics from the original. Statistical resampling techniques can allow for more accurate estimates on the returns of rare events, such as returns of tropical cyclones, provided the underlying distributions are stationary. In contrast, our approach accounts

TABLE 1. Description of variables in the wind field model and their dependence.

Variable:	V	$R_{\rm max}$	p_t	ϕ_t	ψ_t	u_t
Depends on:	$R_{\max}, \phi_t, p_t, u_t$	ϕ_t and sampled	Historical data	Historical data	Historical data	$(\phi_{t,t-1},\psi_{t,t-1})$

for observed nonstationarity in the statistical parameters of the central pressure minima of historical tropical cyclones with longer lifetimes ($T \ge 150 \text{ h}$).

Trends in frequency and intensity of hurricane events have been observed throughout the literature, informed by both historical data and generated data coming from complex climate models, such as general circulation models (GCMs) of the atmosphere. Results described in Keim et al. (2004) indicate that there is strong evidence of an increase in the number of very powerful storms over the past 50-100 years in the North Atlantic Ocean basin and the Gulf of Mexico, after the inclusion of both ENSO and the North Atlantic Oscillation. This claim is supported by historical data and agrees well with results from GCMs under global warming conditions. In addition, marginal trends in central pressure have been noted as far back as 1995 (Hirsch et al. 2001). We find complementary results with regard to increases in the rate of returns of hurricane events with longer lifetimes and trends in central pressure minima. We refer the reader to Keim et al. (2004) for a nice introductory review of the past literature on trends in frequency and power of tropical storms.

Our revised model results in two major differences in the simulation of coastal risk analysis of hurricane events: 1) higher maximum wind speeds are expected for all regions along the North Atlantic coast, including the Gulf Coast, and 2) the highest maximum wind speeds are expected to occur along the northeast seaboard. Higher maximum wind speeds are likely due to a combination of the central pressure minima time dependence and increase in the number of observed hurricane events incorporated into the model. The second observation is arguably more surprising since the number of hurricane events hitting the coast in the north is much lower than regions near the Gulf of Mexico. An increase in the translational velocity as hurricanes travel northward explains this effect.

A recent investigation using the HURDAT2 database also finds an expected increase in returns of extreme wind speeds along the North Atlantic coast; however, this study assumes a fixed warming effect in the surrounding ocean and estimates returns from data-based relationships of extreme wind speed with sea surface temperature so that returns are estimated in a stationary setting (Trepanier 2020).

2. Method

a. The wind field model, maximum wind speeds, and minimum pressure

We describe the wind field model introduced in NOAA (1972) and the relationship between maximum wind speeds and minimum central pressure. Given the center location (ϕ_t, ψ_t) in the usual geographic coordinates (degrees latitude and longitude, respectively) and central pressure p_t in hectopascals of a hurricane measured at the eye at time t, the wind field model allows us to model the stochastic process of maximum

wind speeds of a hurricane as a sequence of random variables sampled at any given time t by

$$V(R_{\text{max}}, \phi_t, p_t, u_t) = 0.865 \left[K \sqrt{\Delta p_t} - \frac{R_{\text{max}}(\phi_t) f}{2} \right] + 0.5 u_t,$$
(1)

where K is a constant [m (s hPa^{1/2})⁻¹], $f = \omega \sin \phi_t$ is the Coriolis parameter $\omega = 7.2982 \times 10^{-4} \text{ s}^{-1}$, $\Delta p_t = 0.75(1013 - p_t)$ is the pressure differential, $R_{\text{max}}(\phi_t)$ is the radius to maximum wind speeds in meters sampled from the distribution in Fig. A2 of appendix A, and u_t is the translational velocity in meters per second at time t. The translational velocity u_t at a time t is estimated as the change in the distance, in meters, of the center of the hurricane

$$\sqrt{(\phi_t - \phi_{t-1})^2 + (\psi_t - \psi_{t-1})^2}$$

over the change in time, in seconds, from time index t-1 to time index t. For more information on how the variables in the wind field model are related see Table 1.

Throughout this article, we will define a hurricane event as a tropical cyclone taking any form (e.g., tropical depression, tropical storm, or hurricane) and denote the total lifetime of a hurricane event as a length of indexed time T representing the total number of 6-h time intervals passed since formation. For any given hurricane event, if we are given the track (ϕ_t, ψ_t) and central pressure time series p_t , we may use Eq. (1) to reconstruct the maximum wind speed $V(R_{\text{max}}, \phi_t, p_t, u_t)$ for all t = 1, ..., T, where t is the index number of 6-h time intervals passed since formation. From Eq. (1) we can see that extreme highs of the maximum wind speed occur for extreme lows of central pressure. Hence, it is important to accurately model the central pressure minima of a hurricane event in order to estimate longer year returns and rare threshold exceedances of maximum wind speeds. Furthermore, central pressure minima often occur at or near landfall so they are particularly important for estimating coastal risk. [We refer to Fig. A1 of appendix A for an illustration of the estimated density plot of central pressure minima occurrence times to landfall times estimated from the tracks of historical hurricane events used in this analysis, which agrees nicely with the density plot found in Casson and Coles (2000, their Fig. 4).]

We can use tools from extreme value theory to model extremes of a time series (e.g., minima or maxima). One well-known strategy is to approximate the set of maxima (or negative minima) taken over blocks of a fixed length m of a set of independent and identically distributed random variables by the GEV given by

$$G(x) = \exp\left\{-\left[1 - \frac{k(x-\mu)}{\sigma}\right]^{-1/k}\right\}$$
 (2)

for x: $1 + k[(x - \mu)/\sigma] \ge 0$, where μ is the location parameter, $\sigma > 0$ is the scale parameter, and k is the shape parameter that defines the tail behavior of G. Under certain regularity conditions, we may use maximum likelihood estimation of the parameters μ , σ , and k to fit the GEV to the block maxima (or negative minima) where each parameter estimate is asymptotically normal provided k > -0.5 (Coles 2001).

By a standard max-stable argument it is not necessary that the block length m be fixed, as long as it is $long\ enough$ so that the maxima (or negative minima) can be modeled by its asymptotic GEV. By the same argument, the GEV that is fit to blocks of varying length is related to G from Eq. (2), with different $\mu = \mu^*$ and $\sigma = \sigma^*$ parameters. A result of this max-stability property is that we may model the central pressure minima of hurricane events coming from historical records with varying lifetimes T. That is, we may model the negative central pressure minima

$$p_{\min} = \min_{t} p_{t} \quad \text{for } t = 1, ..., T$$
 (3)

by the GEV provided the lifetime of each hurricane event is long enough. We will refer to $t_{p_{\min}}$ as the time in the total lifetime of the hurricane event that the central pressure minimum is reached.

We can relax the requirement of strict independence for the GEV in (2) provided the time series is weakly dependent and stationary; see, for example, Leadbetter et al. (1983, chapter 3) or Lucarini et al. (2016). Using historical recordings from the HURDAT2 database, we find that the central pressure minima have the same dependence as in Casson and Coles (2000) on the lifetime T and the latitude $\phi_{t_{p_{\min}}}$ where the central pressure minima occurs. (Figure C1 in appendix C depicts scatterplots of the central pressure minima against the lifetime T and latitude $\phi_{t_{p_{\min}}}$ for landfalling and nonlandfalling hurricanes.)

We limit our model to hurricanes with lifetimes $T \ge 25 =$ 150 hours to ensure convergence of the negative central pressure minima to a GEV distribution. See, for example, the description in Coles (2001, chapter 5.3.1) on GEV models of block maxima or Leadbetter (1974) for estimates on convergence rates of stationary sequences X_{η} to the GEV, where we assume a convergence rate of $O(\eta^{-r})$ for some $r \ge 1$ due to the natural boundedness of central pressure (i.e., central pressures are assumed not to be able reach infinity). There are 642 hurricane events over 1851-2019 in the HURDAT2 database that satisfy this requirement (300 landfalling and 342 nonlandfalling). Central pressure minima from 1851 to 1960 are often recorded for a single time index t along the lifetime of the hurricane event. The corresponding tracks of these hurricane events are estimated using a best tracks procedure (NOAA 1972). While the accuracy of recording the exact central pressure minima would be influenced by the number of locations available to measure central pressure along the track, and hence be lower for these years, we remark that the central pressure minima were often recorded near landfall where we observe the highest chance of central pressure minima occurring over all years (1851–2019). Still, in light of the possibility of data-measuring inaccuracies in early year recordings

(1851–1960), it would be interesting to apply our methods, outlined here for the HURDAT2 historical dataset, to the recently generated STORM dataset in a future investigation (Bloemendaal et al. 2020).

We use maximum likelihood estimation on the parameters of the locally stationary GEV model proposed in Casson and Coles (2000). Although the central pressure minima p_{\min} are sampled from independent hurricane events, they have some underlying dependence on both the lifetime T and latitude $\phi_{t_{p_{\min}}}$ of the hurricane event, which is accounted for in the location μ and scale σ parameters of this locally stationary model. We find poor fits for quantile plots of this locally stationary model.

A natural question is whether there exists some time dependence in the distribution of central pressure minima.

b. A nonstationary model for central pressure minima

We investigate the time dependence in the location μ and scale σ parameters of central pressure minima for landfalling and nonlandfalling hurricanes. As a preliminary investigation, we split the central pressure minima into two parts, central pressure minima of hurricane events occurring between 1851 and 1980 and those occurring between 1981 and 2019 and then test whether a statistically significant change in the statistical parameters is observed. We perform an F test for equal variance that indicates the variance of the central pressure minima for landfalling hurricanes has significantly changed (p = 0.004)in the last 40 years. We obtain a similar result using a t test for equal means of the central pressure minima for nonlandfalling hurricanes (p = 0.012). Normality assumptions for the t test are met by a moderately large sample size and the central limit theorem, 176 and 166 nonlandfalling hurricanes over 1851-1980 and 1981-2019, respectively. On the other hand, results from the F test are reasonably robust against nonnormality provided our sample sizes are similar and moderately large (Donaldson 1966), 166 and 134 landfalling hurricanes over 1851–1980 and 1981–2019, respectively. Preliminary investigations into the time dependence of the shape k parameter showed no obvious trend, so it is taken as constant.

Motivated by the observed difference in the statistical parameters of the central pressure minima in the last 40 years, we now investigate the possibility of a time-dependent trend in the location and scale parameters of the locally stationary model proposed by Casson and Coles (2000). This locally stationary model asserts a dependence of the location μ and scale σ parameters on the lifetime T of the hurricane and latitude $\phi_{t_{p_{\min}}}$ of the central pressure minima. We use this model as a basis for checking the time dependence of the μ and σ parameters in the GEV described by Eq. (2). We begin by performing maximum likelihood estimation of all the coefficient parameters used in the locally stationary model. Maximum likelihood estimation is performed on subsets of the 300 (similarly, 342) historical values of central pressure minima from landfalling (similarly, nonlandfalling) hurricanes taken over moving time windows of 40 years with a time step of 1 year by maximizing the negative log-likelihood of the locally stationary GEV defined by

$$\ell_{t_{yr},T,\phi_{t_{p_{\min}}}}(p_{\min}) = -h\log\sigma(T,\phi_{t_{p_{\min}}}) - [1 + (1/k)]$$

$$\times \sum_{i=1}^{h}\log\left\{1 + k\left[\frac{p_{\min,i} - \mu(T,\phi_{t_{p_{\min}}})}{\sigma(T,\phi_{t_{p_{\min}}})}\right]\right\}$$

$$- \sum_{i=1}^{h}\left\{1 + k\left[\frac{p_{\min,i} - \mu(T,\phi_{t_{p_{\min}}})}{\sigma(T,\phi_{t_{p_{\min}}})}\right]\right\}^{-1/k}, \quad (4)$$

where $t_{yr} = year - 1851$ and h is the number of central pressure minima $p_{\min,i}$ occurring in the 40-yr window $[t_{yr}, t_{yr} + 40]$. We choose 40-yr windows because 1) we observed a statistically significant difference in the location and scale parameters over the last 40 years and 2) 40 years of central pressure minima is a long enough period to obtain reasonable confidence intervals (ci) around our maximum likelihood estimates. Our final result is a set of time series representing the maximum likelihood values of the coefficient parameters in the locally stationary model. We then reconstruct the time series of the location, $\mu(t_{\rm vr})$, and scale, $\sigma(t_{\rm vr})$, using the relationships described in the locally stationary model and the historical values of T and $\phi_{t_{p_{\min}}}$. From now on, we will refer to the time series $\mu(t_{\rm yr})$ and $\sigma(t_{\rm yr})$ as the location time series and scale time series, respectively, to differentiate between the other time series in this investigation.

For each 40-yr window, the set of lifetimes T and locations $\phi_{t_{p_{\min}}}$ of historical hurricane events occurring in the 40-yr window are used to estimate the coefficients of the locally stationary model described in Eqs. (B1) and (B2) of appendix B for landfalling and nonlandfalling hurricanes, respectively. Since the location time series for the nonlandfalling case has a dependence on the lifetime, T, we fix such a T to construct the location time series, which results in 342 location time series taken from the 342 fixed values of historical recordings of T (one for each hurricane event). This is in contrast to the scale parameter of landfalling hurricanes, which does not have a dependence on T or $\phi_{t_{p_{\min}}}$ and, as a consequence, results in a single scale time series.

Unreliable maximum likelihood estimates of the location and scale parameters in the years 1851–1960 are found and are due to low numbers of recorded hurricane events with lifetimes $T \ge 25$ where the yearly average over this time period is 1.324. Nevertheless, continuous time-dependent trends are noticeable after 1960 for parameters in both the landfalling and nonlandfalling case.

To determine whether a trend is reliable, we perform the Mann–Kendall test for trend on all the location and scale time series. We find a positive statistically significant trend for the scale parameter in the landfalling case and a negative statistically significant trend for all time series of the location parameter in the nonlandfalling case. Trends were evaluated using the Kendall correlation coefficient τ_b with 95% confidence intervals calculated following (Hollander et al. 2015, chapter 9.3). The Kendall correlation coefficient is estimated for all years and for years from 1960 to 2020, for comparison. For an illustration of the trend results and

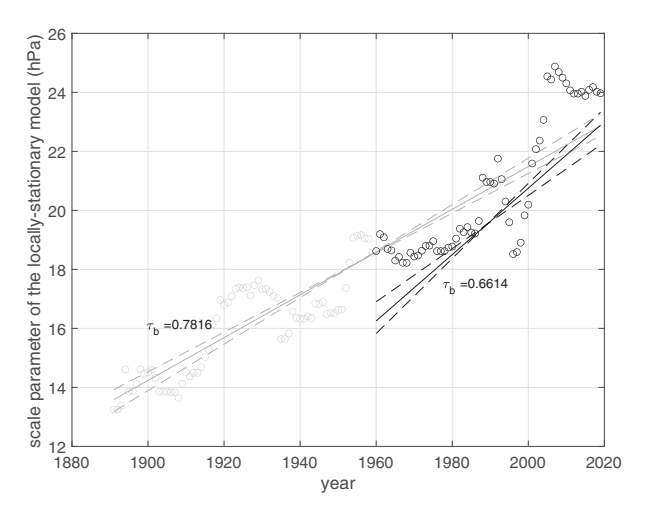


FIG. 1. Time series of parameter $\sigma(t_{yr}) = \sigma_0(t_{yr})$ coming from the stationary model for $-p_{\min}$ (hPa) of landfalling hurricanes constructed from likelihood estimates. The value τ_b is the Kendall correlation coefficient. The x axis represents the end year of the 40-yr time window chosen for likelihood parameter estimation. Dark circles highlight the maximum likelihood estimates of the $\sigma(t_{yr})$ parameter after 1960 (end year) when the quantity of recorded hurricane events in the 40-yr time window produce reliable maximum likelihood estimates. Crossover of 95% confidence intervals of τ_b , indicated by a dashed line, is a result of choosing the median as the intercept for plotting.

parameter time series see Figs. 1 and 2, respectively. We do not find clear evidence for a reliable trend in the location time series for the landfalling case or the scale time series for the nonlandfalling case.

From these results, we propose the following nonstationary model (t_{yr} = year – 1851 is the yearly index):

$$\mu = \mu_0 + \mu_1 \log(T) + \mu_2 \phi_{t_{\text{Pmin}}}, \quad \sigma = \sigma_0 + \sigma_1 t_{\text{yr}}, \quad k = k_0,$$
(5)

for landfalling hurricanes, and

$$\mu = \mu_0 + \mu_1 \log(T) + \mu_2 \log(t_{\text{yr}}), \quad \sigma = \sigma_0 + \sigma_1 \phi_{t_{\text{p}_{\min}}},$$

$$k = k_0, \tag{6}$$

for nonlandfalling hurricanes. Maximum likelihood estimates from the negative log-likelihood of Eq. (2), with location and scale parameters given by Eqs. (5) and (6), and standard errors (se) estimated from the information matrix are provided in Table 2. We find using the likelihood ratio test (LRT) that our revised nonstationary model for central pressure minima offers a statistically significant better fit to the data than the stationary model with test statistics well beyond $\Lambda_{0.05,1} = 3.84$, the statistic corresponding to the $\alpha = 0.05$ significance level with 1 degree of freedom (see Λ in Table 2).

Results from Kim et al. (2017) indicate that for sample sizes of greater than 40 (ours is on the order of 300 for each model), the LRT has the best performance across other model methods [Akaike information criteria (AIC), corrected

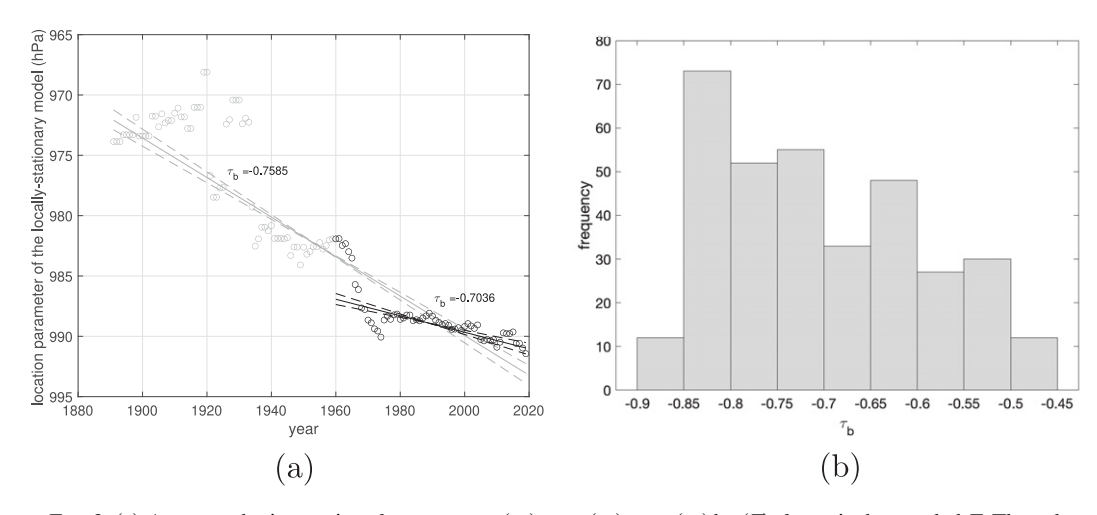


FIG. 2. (a) An example time series of parameter $\mu(t_{yr}) = \mu_0(t_{yr}) + \mu_1(t_{yr}) \log(T)$, for a single sampled T. The value τ_b is the Kendall correlation coefficient. The x axis represents the end year of the 40-yr time window chosen for likelihood parameter estimation. Dark circles highlight the maximum likelihood estimates of the $\mu(t_{yr})$ parameter after 1960 (end year) when the quantity of recorded hurricane events in the 40-yr time window produces reliable maximum likelihood estimates. (b) The τ_b for all time series of $\mu(t_{yr})$, illustrating that all time series have a statistically significant negative Kendall correlation coefficient. Crossover of 95% confidence intervals of τ_b , indicated by a dashed line, is a result of choosing the median as the intercept for plotting.

AIC (AICc), and Bayesian information criterion (BIC)] to appropriately estimate the nonstationary GEV with time-varying location parameter while the AIC performs better for time-varying location and scale parameters; however, the authors state that they expect the AIC outperforms other methods because of its tendency to select more complex models. Informed by the preliminary investigation into the time dependence of location and scale parameters in the data, we did not see a reason to increase the complexity of our model. It would be interesting to investigate the possibility of using the AIC for future models where there is evidence for multiple time-varying parameters in our GEV model.

c. Poisson returns of hurricane events and a nonstationary rate parameter

We investigate a Poisson model for yearly returns of hurricane events where the number of expected yearly hurricane events is increasing over time.

Returns of extreme hurricane events, such as low central pressure minima or high maximum wind speeds, are often reported in terms of an *n*-yr return. To interpret returns in this way, our model must consider how often a hurricane event occurs in a given year. Classically, it is expected that a rare event, such as a hurricane, is modeled by a Poisson distribution given by

$$P(X = \mathcal{K}) = \frac{\lambda^{\mathcal{K}} e^{-\lambda t}}{\mathcal{K}!},\tag{7}$$

where $\lambda = r/t$ is the rate parameter estimated as the number of events r in a given time t.

Under the assumption of stationarity, the authors in Casson and Coles (2000) estimate a fixed rate parameter, $\lambda = 5.45$ hurricane events per year, as the average number of returns of a hurricane in a given year over 1965–94. With more data available in the HURDAT2 database, we are able to estimate the time-dependent yearly rate parameter $\lambda_{t_{yr}}$ over 20-yr sliding windows from 1851 to 2019. We refer the reader to Fig. 3 for an illustration of the estimated yearly rate parameter.

We fit an exponential to the time-dependent Poisson rate parameter $\lambda_{t_{y_t}}$ by maximizing the negative log-likelihood function with respect to parameters a and b of our exponential model,

$$\lambda_{t_{\rm yr}} = ae^{bt_{\rm yr}}.\tag{8}$$

Maximum likelihood estimates and confidence intervals of *a* and *b* can be found in Table 3. Our model for hurricane returns does not differentiate between landfalling and nonlandfalling hurricane events due to the nature of the simulation in

TABLE 2. Maximum likelihood estimates of the parameters in the nonstationary generalized extreme value distribution model for $-p_{\min}$. Time-dependent parameters are marked with an asterisk. Likelihood ratio test statistics for our revised nonstationary model of $-p_{\min}$ against the stationary model are indicated by Λ .

Туре	μ_0 (se)	μ ₁ (se)	μ ₂ (se)	σ_0 (se)	σ_1 (se)	k (se)	Λ
Landfalling	-1078.97 (14.48)	32.87 (3.60)	-0.52(0.16)	12.47 (1.86)	$0.07 (0.02)^*$	-0.13 (0.04)	15.62
Nonlandfalling	-1027.13 (13.65)	27.40 (2.76)	$-11.47 (1.84)^*$	20.48 (2.04)	-0.16 (0.06)	-0.13(0.04)	30.77

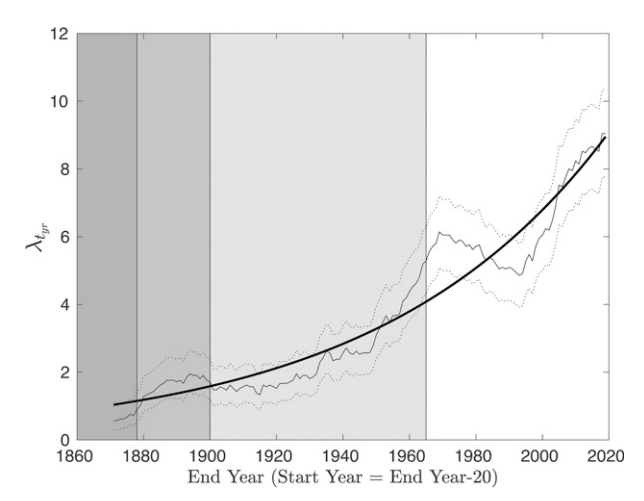


FIG. 3. Maximum likelihood estimate of the Poisson parameter for yearly hurricane event rates with lifetimes greater than 6.25 days. Estimates are taken over 20-yr moving time windows. Standard errors are marked with dotted lines. The fitted exponential model is represented by a thick line. Grayed areas correspond to those in Vecchi et al. (2021): 1) 1878—year when the U.S. Signal Corps began cataloging all Atlantic Ocean hurricanes; 2) 1900—year when the U.S. coast was sufficiently well populated for monitoring; 3) modern era with appropriate ship density.

the final section. This is because tracks of a simulated hurricane are generated by randomly sampling a historical track and adding noise. To compare our results with current literature, we separate the discussion of returns of hurricane events for landfalling and nonlandfalling hurricanes in the paragraphs below.

There is some debate on whether the average number of hurricane events is increasing generally; some literature suggests that low ship density is the underlying cause for the low number of recorded hurricanes for years up to 1965 (Landsea et al. 2010; Vecchi and Knutson 2010), while others report significant increases in frequency after the late 1980s (Vecchi and Knutson 2007). When averaging yearly frequency over moving time windows, the authors in Vecchi and Knutson (2007) report a small nominally positive upward trend post-1878. The work of Landsea et al. (2010) finds an increase in the occurrence of short lifetime hurricanes only, leading the authors to conclude ship density as a plausible cause for the observed trend. It is important to note that the literature described here uses the retired HURDAT database for their analyses rather than the HURDAT2 database used in this investigation; however, this certainly does not rule out the possibility of historically unrecorded storms in the updated database. There is active research on the frequency of hurricane events recorded in the HURDAT2 database where an observed late-twentieth-century trend is attributed to a possible unusually low minima in the 1980s (Vecchi et al. 2021).

We find an increasing trend in frequency of hurricane events longer than 6.25 days using the Poisson rate parameter, which differs from the results in Landsea et al. (2010).

TABLE 3. Maximum likelihood estimates and 95% confidence intervals of the exponential model for the time-dependent Poisson parameter $\lambda_{t_{\rm vr}}$.

a (ci)	b (ci)
1.024 (0.925, 1.123)	0.015 (0.014, 0.015)

This trend holds even into the modern era (post-1965) where ship density is expected to remain steady. One explanation for this difference could be our use of a Poisson rate estimate over a moving average. Rate estimates expect that an increase in the mean results in an increase in the variance. This phenomenon is observed in the raw data. In the case of a moving average estimate this increase in variance can cause statistical tests of the mean difference to be near zero due to large standard errors. We also do not separate hurricane events by wind speed where differences in trend have been reported (Vecchi and Knutson 2007). Since we limit our investigation to hurricanes with life-spans longer than 6.25 days, our findings may also be a result of some underlying increase in the life-span of hurricane events as a whole. Using the yearly estimates from our model for the rate over 1965-94 we find that the average is identical to past literature, which provides some reasonable benchmark (Casson and Coles 2000).

An argument could be made that this increase in the total number of observed hurricane events post-1965 comes from our ability to more readily observe nonlandfalling hurricanes. However, an increase in the Poisson rate parameter is also observed for strictly landfalling hurricane events of lifetimes longer than 6.25 days; however, this rate parameter follows a similar pattern (with low minima in the 1980s) to that of Vecchi et al. (2021) with a slight increase in the current peak relative to that of 1965.

d. Verification of the nonstationary model for central pressure minima

We use a combination of established statistical methods to illustrate the reliability of our nonstationary model at predicting returns of central pressure minima.

To test the reliability of our model to accurately predict the distribution of central pressure minima without updating, we break the HURDAT2 database up into a *training* set, which we will use to simulate hurricanes from the model and *test* set, which we will use to compare risk probability outcomes estimated from the training set with the "true" probabilities. Our training set will be defined as the set of all years in our dataset minus the number of years *n* used to obtain the *n*-yr returns and our test set will be the *n* last years in our dataset. For example, if we are interested in finding the 50-yr returns, our training set would be defined as the set of all hurricanes occurring between 1851 and 1970 and our test set would be the set of all hurricanes occurring between 1971 and 2019.

Under the assumption that our negative central pressure minima follow some generalized extreme value distribution, [Coles 2001, section 6b(c)] suggests the use of

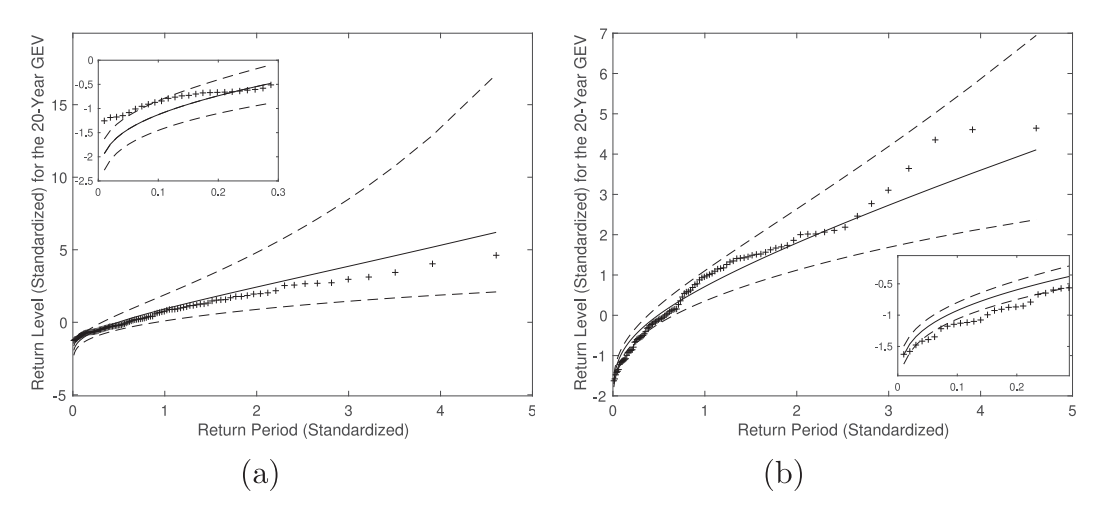


FIG. 4. Return levels and periods of the 20-yr nonstationary GEV using the standardized $-p_{\min}$ coming from Eq. (9) for (a) nonlandfalling and (b) landfalling hurricanes. Solid lines and dashed lines represent the model and 95% confidence intervals approximated from the training set over 1851–2000. A plus sign indicates the true return levels calculated from the test set over 2001–19. Return periods and return levels here are based on Eq. (9), are nondimensional, and are expected to follow the Gumbel distribution (10).

a sequence of standardized variables $\boldsymbol{z}_{t_{\mathrm{yr}}}$ defined for our purposes by

$$z_{t_{yr}} = \frac{1}{k} \log \left\{ 1 + k \left[\frac{-p_{\min}(t_{yr}) - \mu(t_{yr})}{\sigma(t_{yr})} \right] \right\}, \tag{9}$$

each having a standard Gumbel distribution,

$$P(z_{t_{m}} \le z) = \exp\{-e^{-z}\}, \quad z \in \mathbb{R}.$$
 (10)

The advantage of using this sequence is that the "true" quantile plots of the observed and standardized $-p_{\min}(t_{\rm yr})$ in the test set can be made with reference to the distribution for the simulated (under the nonstationary model) and standardized $-p_{\min}(t_{\rm yr})$ from the training set.

We generate data to model negative central pressure minima n-yr returns for the years in the test set using 1) the parameter likelihoods of $\mu(t_{yr})$, $\sigma(t_{yr})$, and k defined by the model in Eqs. (5) and (6) estimated from the training set and 2) the appropriate rate parameters defined by Eq. (8) to compute returns of hurricane events using Eq. (7) where t_{yr} indices are chosen to correspond to those of the test set. By way of the model, the generated central pressure minima follow a nonstationary distribution.

We are interested in whether the central pressure minima generated from our nonstationary model with parameters estimated by central pressure minima from the training set accurately represent the historical central pressure minima we have in the test set. We cannot directly compare the model and historical values because of the nonstationarity we observe; however, we can perform a comparison by standardizing the model and historical central pressure minima using Eq. (8). Provided the model with estimated $\mu(t_{yr})$ and $\sigma(t_{yr})$ appropriately describes the nonstationarity we observe, the

standardized historical central pressure minima, denoted by $z_{t_{yr}}$ in Eq. (9), will follow the Gumbel distribution described by Eq. (10).

We use this data to compute the model standardized quantile plots for 20-, 30-, and 50-yr return periods given by quantiles of the standard Gumbel distribution (Coles 2001, section 3.4),

$$z_{q} = \mu - \sigma \log[-\log(1 - q)], \tag{11}$$

for both landfalling and nonlandfalling hurricanes, where $\mu=0$, $\sigma=1$, and z_q is the return level associated to the return period 1/q. Figures 4, 5, and 6 show model results against the actual data in the test set. Not surprisingly, better approximations for both the landfalling and nonlandfalling case are made for shorter n-yr returns; however, estimates for 50-yr returns still fall reasonably within the 95% confidence interval of the model estimated from the information matrix.

Using the standardized negative central pressure minima allows us to estimate the accuracy of the nonstationary model against true data; however, it does not provide us with a complete way of interpreting the n-yr returns. At best, we are able to fix a year index t_{yr} and state the probability of the negative central pressure minima being above a certain threshold in that given year. Most risk analysis involves directly computing n-yr return levels where a new definition needs to be introduced in the nonstationary setting. We discuss this in detail in the next section.

3. Application of method for coastal wind speed risk

a. Time-dependent returns of high maximum wind speeds

In this section, we discuss a definition for time-dependent *n*-yr return levels of maximum wind speeds.

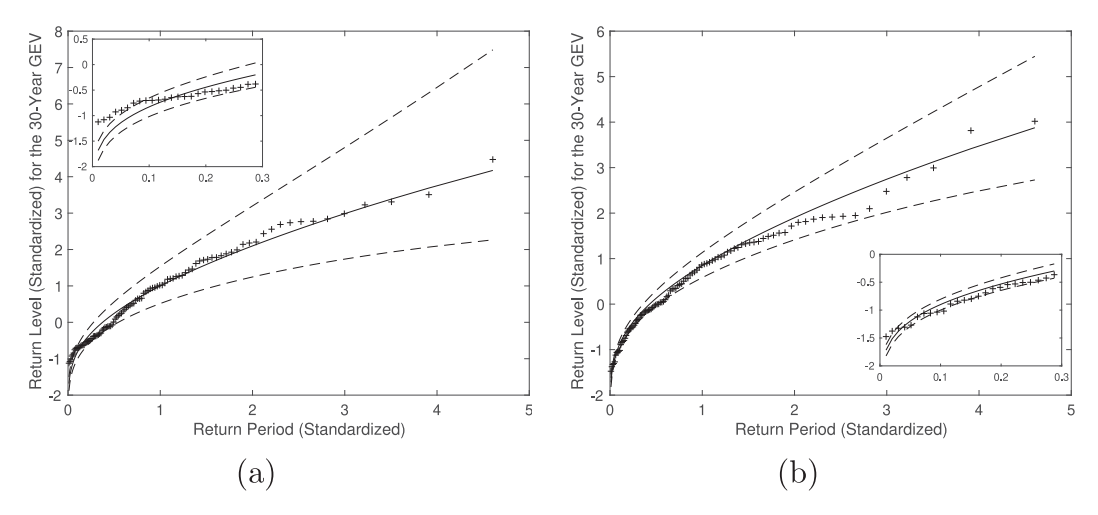


Fig. 5. As in Fig. 4, but of the 30-yr nonstationary GEV. Solid lines and dashed lines represent the model and 95% confidence intervals approximated from the training set over 1851–1990. A plus sign indicates the true return levels calculated from the test set over 1991–2019.

Return level is often used in risk analysis to communicate the threshold that we are expected to exceed in a given amount of time. For example, we may ask what is the maximum value of the wind speed that we are expected to exceed in *n* years. When accounting for nonstationary effects, such as those brought on by climate change, the probability of observing values above or below a threshold varies over time so that terms like return level no longer make physical sense. We refer the reader to Salas and Obeysekera (2014) for a nice description of current definitions of return probabilities in the nonstationary setting.

Cooley (2013, section 4b) introduces the idea of extending the definition of the *n*-yr return level to the nonstationary

case by taking the threshold where the expected number of exceedances in n years is 1. In the context of nonstationary wind speed prediction this would be equivalent to solving for r_n in

$$1 = \sum_{t_{vr}=1}^{n} [1 - F_{t_{yr}}(r_n)], \tag{12}$$

where r_n is the *n*-yr return level beginning with year $t_{yr} = 1$ and ending with year $t_{yr} = n$ and $F_{t_{yr}}$ is the unknown indexed yearly cumulative distribution function of maximum wind speed. For example, if we are interested in finding the 50-yr return level r_{50} of wind speed, Eq. (12) would become

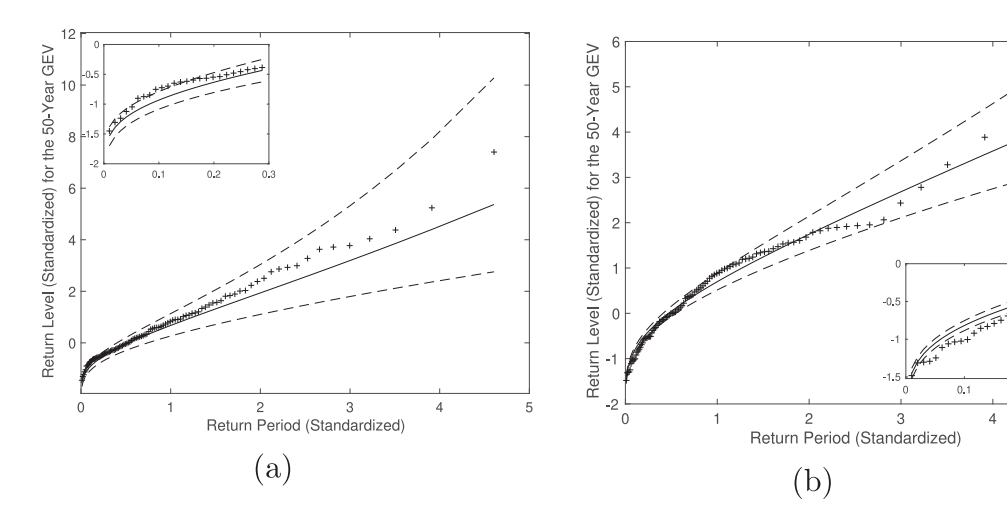
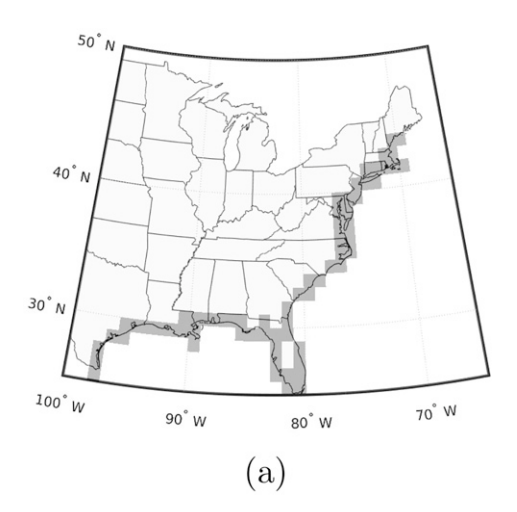


FIG. 6. As in Fig. 4, but of of the 50-yr nonstationary GEV. Solid lines and dashed lines represent the model and 95% confidence intervals approximated from the training set over 1851–1970. A plus sign indicates the true return levels calculated from the test set over 1971–2019.



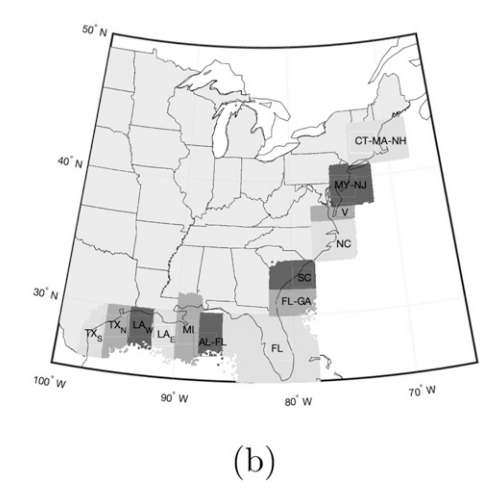


FIG. 7. (a) Coarse grid representing the coastal line. (b) Simulated hurricane locations along the coastal line. Different regions are indicated in grayscale.

$$1 = \sum_{t_{yr}=1}^{50} [1 - F_{t_{yr}}(r_{50})] = P_1(ws > r_{50}) + \dots + P_{50}(ws > r_{50}).$$
(13)

The corresponding n-yr return level can be numerically estimated for future years by extrapolating the trend in the model and approximating r_n by calculating the 1 - (1/n) quantile of the equal weight mixed probability density function of wind speed occurring over $t_{\rm yr} = 1, \ldots, n$ years given by

$$f(x;t_1,...,t_n) = \sum_{t_{v_x}=1}^{n} f_{t_{v_x}}(x),$$
 (14)

where $f_{t_{yr}}$ is the unknown and numerically approximated probability density function of the wind speed corresponding to the yearly time index t_{yr} . In fact, the definition in Eq. (14) has also been used to model regional returns of extremes where $f(x; \ell_1, \ldots, \ell_n)$ varies by location ℓ_i instead of time (Carney and Kantz 2020).

b. A Simulation to estimate maximum wind speed risk along the U.S. North Atlantic coast

We run a simulation using the adaptations described in earlier sections to estimate high maximum wind speed risk for specified regions along the U.S. North Atlantic coast.

From the wind field model described in Eq. (1), we observe that returns of low central pressure minima have a large and direct effect on returns of high maximum wind speeds. This relationship makes appropriately modeling central pressure minima vital when considering returns of extreme wind speeds along the coast. However, it is not enough to know the central pressure minima to estimate coastal wind speed risk. This is because maximum wind speeds for a coastal region depend, among other things, on the translational velocity of the hurricane, the location at which landfall occurs, and whether the central pressure minimum is achieved at landfall.

We now consider a more complex hurricane simulation to estimate the unknown distribution described in Eq. (14) of maximum wind speeds for a particular coastal location with the adaptations described in this investigation. The simulation is outlined in appendix A; however, we refer the reader to the original literature (Casson and Coles 2000) for a detailed description. In essence, the process described in appendix A simulates a series of hurricane events for a given year by sampling the number of events to occur and the random variables used in the wind field model represented by Eq. (1) at each time t along a simulated hurricane track. Once all hurricane events for a set of years have been simulated, we sample the wind speed for each simulated hurricane landing along a specified coastline to form the unknown distribution described in Eq. (14). The North Atlantic coastline is first approximated by a coarse grid, illustrated in Fig. 7, then divided into coastal regions: north Texas, south Texas, west Louisiana, east Louisiana, Mississippi, Alabama-Florida, Florida, Florida-Georgia, South Carolina, North Carolina, Virginia, Maryland-New Jersey, and Connecticut-Massachusetts-New Hampshire. A simulated hurricane is said to be "on the coast" if the eye of the hurricane is within 2° of the coastal line.

To estimate the *n*-yr return levels for regions along the coast, we must numerically approximate the probability distribution function of wind speeds described in Eq. (14). Then the *n*-yr return level is simply the 1-(1/n) quantile of the combined frequency distribution of maximum wind speed data for each coastal region. We do this for 20-, 30-, and 50-yr return levels for each region taken along the coast by generating 20, 30, and 50 years of data (i.e., 2020–40, 2020–50, and 2020–70) for N=1000 trials and estimating the 0.95, 0.97, and 0.98 quantiles, respectively. It is reasonable to assume that each likelihood parameter in our simulation of maximum wind speeds (there are several) θ has reached its asymptotic normal distribution $\mathcal{N}(\hat{\theta}, s_{\theta})$ with mean $\hat{\theta}$ equal to the maximum likelihood estimate of the parameter θ and standard deviation given by the standard error s_{θ} approximated from the

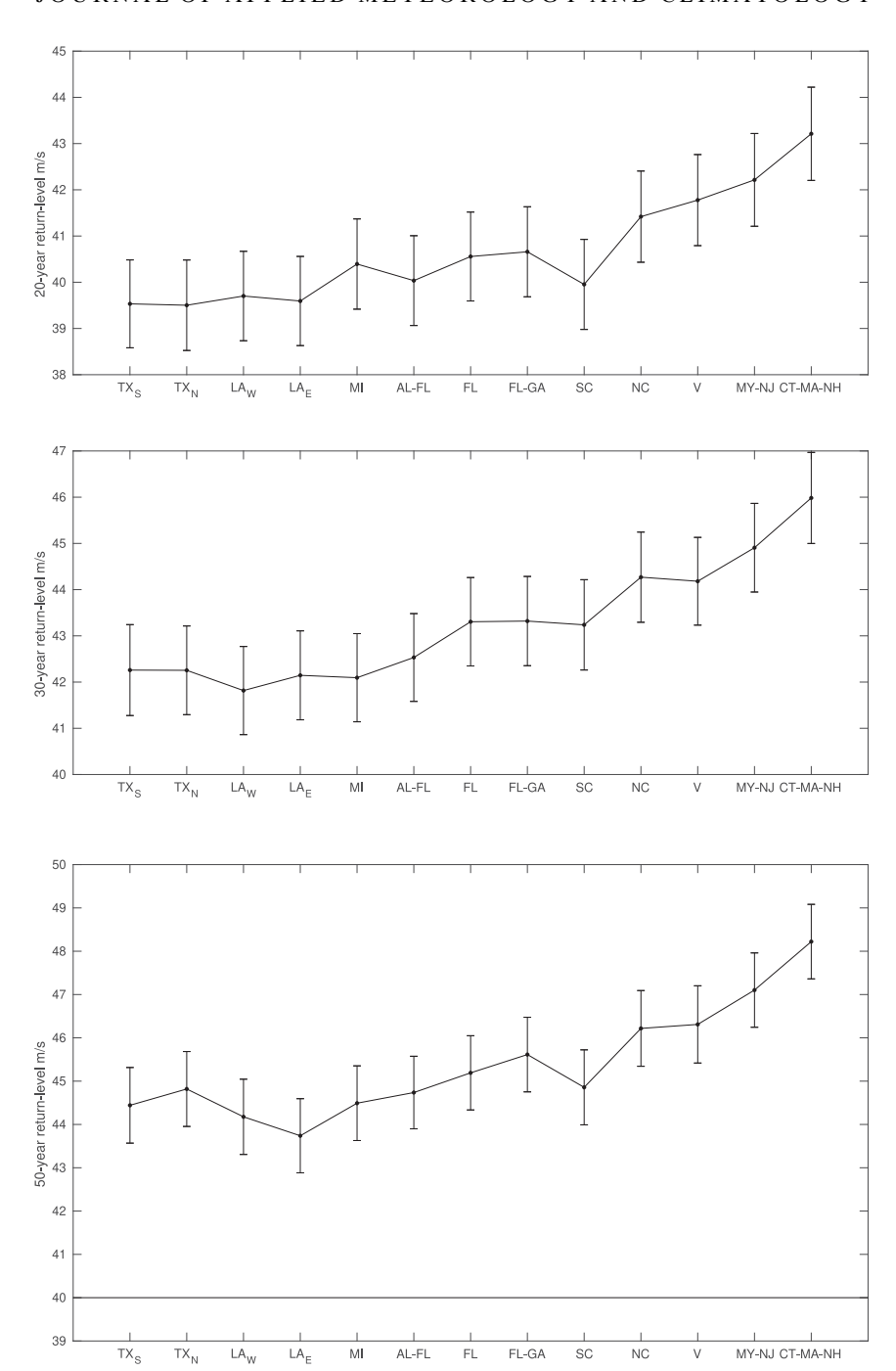


FIG. 8. Plots of the (top) 20-, (middle) 30-, and (bottom) 50-yr return levels of maximum wind speed along the coast estimated for 2021. Central estimates are the quantiles of the distribution of 6-hourly wind speeds for N=1000 trials of 20, 30, and 50 years of simulated hurricanes, respectively. Error bars represent the 95% confidence interval estimates from Eq. (15). The solid horizontal line indicates the maximum wind speed return estimated from stationary models of previous literature.

Hessian. We can be confident that the true population distribution of maximum wind speeds, which the model is meant to represent, falls within some combination of these parameters; each coming from their corresponding distribution $\mathcal{N}(\hat{\theta}, s_{\theta})$.

To estimate the confidence intervals of maximum wind speed return levels, we independently sample from each of the parameter distributions to obtain 100 different combinations of parameters. We then run the simulation with each set

of parameters for 2000 (e.g., 20 years and N=100 trials), 3000 and 5000 years of hurricane simulations and estimate the 20-, 30-, and 50-yr return levels. Given that each of these simulations is independent, we are left with a sequence of quantile estimates (return levels) coming from an independent and identically distributed (i.i.d.) sequence of maximum wind speeds for each coastal region. It is shown in Knight (2002) that quantiles coming from i.i.d. sequences can be well approximated by a normal distribution. Confidence intervals of each return level are then estimated by assuming an underlying normal distribution so that

$$CI_{0.95} = \left[F_{\text{norm}}^{-1}(0.025) \frac{\sigma_q}{\sqrt{100}}, F_{\text{norm}}^{-1}(0.975) \frac{\sigma_q}{\sqrt{100}} \right],$$
 (15)

where $F_{\rm norm}^{-1}$ is the inverse standard normal distribution and σ_q is the estimated standard deviation of the 100 quantiles obtained from the 100 different parameter combinations. Quantiles to estimate 20-, 30-, and 50-yr return levels of maximum wind speed for each coastal region and their 95% estimated confidence intervals can be found in Fig. 8.

4. Discussion

The wind field model (NOAA 1972) has provided a convenient way of calculating the maximum wind speed of a hurricane event at any given time along a track, provided the central pressure is known. According to this model, high maximum wind speeds are obtained for low central pressure measurements. It is shown in Casson and Coles (2000) that this relationship can be used as a guide for estimating returns of extremely high maximum wind speeds along the coast by appropriately modeling the pressure minima. They found using the HURDAT database that central pressure can be modeled by the generalized extreme value distribution with stationary location and scale parameters depending on the lifetime and latitude of the central pressure minima. The simulation results of Casson and Coles (2000) using a stationary model of central pressure minima are in good agreement with the other models and analyses of the decade (Batts et al. 1980; Ho et al. 1987). However, our investigation shows that this stationary model does not appropriately fit the central pressure minima of the updated HURDAT2 database. These poor fits can be almost entirely blamed on a time-dependent component of the scale and location parameters in the model. We have proposed a new, nonstationary model that accounts for this observed time dependence in the location and scale parameter of the central pressure minima. Our model shows very reasonable fits to the true central pressure minima. Following a standard approach, we assume a Poisson distribution for yearly returns of hurricane events; however, we show that this model is also time dependent with an exponentially increasing rate parameter for hurricane events with lifetimes greater than 6.25 days. We discuss this against current literature where stationarity of hurricane returns is assumed. We show that our models can reliably predict up to at least 50-yr returns for the central pressure minima without the need for

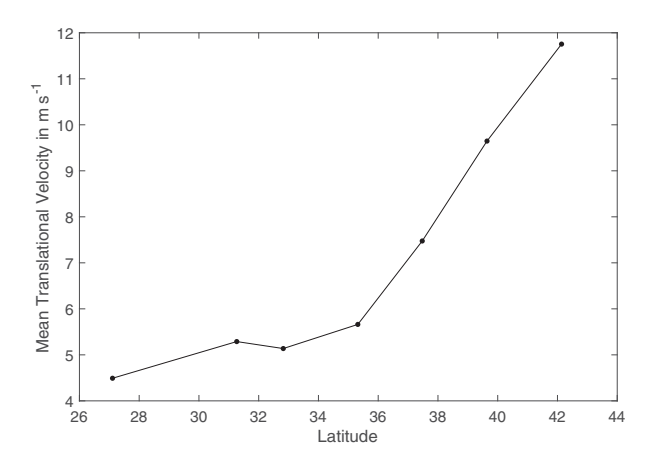


FIG. 9. Average translational speed for simulated hurricanes from our model along the coast plotted against latitude.

updating by comparing the generated training-set model against a test set and standardizing the central pressure minima using extreme value methods.

We have used our nonstationary model of central pressure minima and Poisson returns for yearly hurricanes in a more complex simulation to estimate 20-, 30-, and 50-yr return levels of maximum wind speeds for sections along the U.S. North Atlantic coastline. In comparison with other analyses of maximum wind speed returns for coastal regions that are based on the HURDAT database such as those in Batts et al. (1980), Coles (2001), and Casson and Coles (2000), our model has two significant results: 1) higher maximum wind speeds are expected for all regions along the U.S. North Atlantic coast, and 2) the highest maximum wind speeds occur along the northeast seaboard.

Specifically for landfalling hurricanes, we find a scale parameter for negative central pressure minima that is linearly increasing with time, which suggests an expectation for higher highs and lower lows of central pressure minima. This phenomenon coupled with a general increase in the observed number of hurricane events can certainly lead to higher maximum wind speeds everywhere along the coast.

An increase in the maximum wind speed for higher latitudes is actually a nontrivial observation because return levels are affected by the number of hurricanes observed in a coastal region. In general, the number of observed hurricanes in the north tend to be lower. For example, it is well known that the coastal region around Florida has many more hurricane events than those regions along the northeast seaboard In fact, we find this to be true in our simulations as well. So, one would expect to have a higher 20-yr maximum wind speed return level for the Florida region than the northeast. On the other hand, translational velocity plays a critical role in the maximum wind speed of a hurricane hitting the coastal region, by definition of the wind field model described by Eq. (1), where translational velocity is always greater for higher latitudes (see, e.g., the translational velocity estimates by latitude in Yamaguchi et al. (2020).

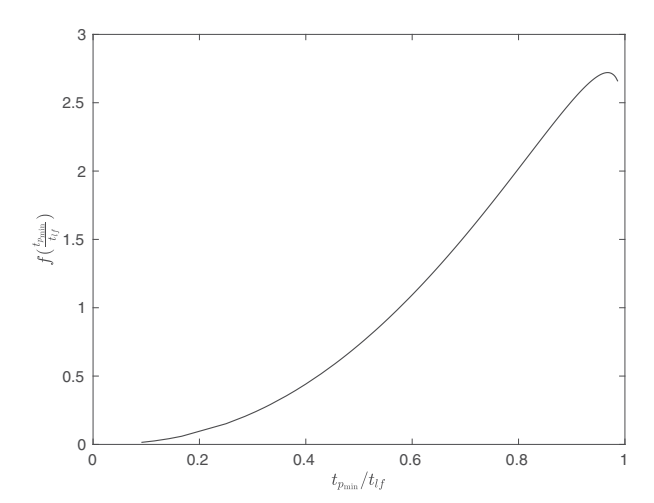


FIG. A1. Empirical density function of the ratio $t_{p_{\min}}/t_{\rm lf}$ for land-falling hurricanes that make landfall after their central pressure minima occur.

We have tested our model to determine the cause of this northern increase in maximum wind speed and have found that translational velocity has the greatest influence over the observed trend. Furthermore, our simulated values of average translational velocity, estimated from the simulated hurricane tracks, almost identically follow those found in the literature (Yamaguchi et al. 2020, their Fig. 2d). We refer the reader to Fig. 9 for a plot of translational velocity over latitude. This result provides us with reasonable confidence in our model for coastal risk analysis.

In line with the ongoing scientific discussion summarized in Knutson et al. (2019), we remark that the nonstationarity of hurricane central pressure minima (and hence, maximum wind speed) detected in this investigation does not allow us to make conclusions on the underlying drivers of such change. It would be an interesting follow-up investigation to consider the contributions of different causal factors, anthropogenic or natural long-term variability arising from effects of El Niño (ENSO) and the North Atlantic Oscillation. Following the work from Patricola and Wehner (2018), we may use the methods described in this investigation with simulated data coming from complex climate models, such as the Weather Research and Forecasting Model, where we can control for CO₂ emission levels. Additionally, we could consider a large generated dataset, such as the STORM dataset from Bloemendaal et al. (2020), with supporting historical CO₂ emission level recordings. We could then investigate contributions of long-term trends to central pressure minima as a control and compare these results with increasing emission levels.

Acknowledgments. Author Carney thanks MPIPKS, where part of this work was completed, for their hospitality. Author Nicol thanks the U.S. National Science Foundation for support on NSF-DMS Grants 1600780 and 2009923.

Data availability statement. The historical central pressure and track data are freely available online from NOAA (https://

TABLE A1. Maximum likelihood estimates of the parameters in the normal distributional model from Casson and Coles (2000, their section 2.5) for $p_{\rm range}$.

Type	a (se)	b (se)	c (se)
Landfalling	872.33 (25.48)	-0.87 (0.03)	11.77 (0.32)
Nonlandfalling	829.50 (19.77)	-0.82 (0.02)	7.47 (0.19)

www.nhc.noaa.gov/data/hurdat/hurdat2-1851-2020-052921.txt; Landsea and Franklin 2013). The code used to perform the nonstationary investigation, model fits, and wind speed simulation was written in MATLAB. Access to the code used in this investigation and a user-interfaced simulation package based on the nonstationary model proposed here can be found online (https://doi.org/10.48610/92ad85c).

APPENDIX A

Numerical Simulation of Maximum Wind Speeds for Hurricane Events

A summary of the scheme for simulating the time series of maximum wind speeds of a yearly sample of hurricane events is presented in this appendix. Adaptations from this investigation are marked with an asterisk. Sampling tracks or time series refers to sampling from the 642 historical hurricane records from the HURDAT2 database. Densities and probabilities are estimated from the 642 historical hurricane records.

The scheme is as follows:

- Sample the number of hurricane events to occur for a specified year from Eq. (7) with the rate parameter in Eq. (8).
- 2) For each hurricane event:

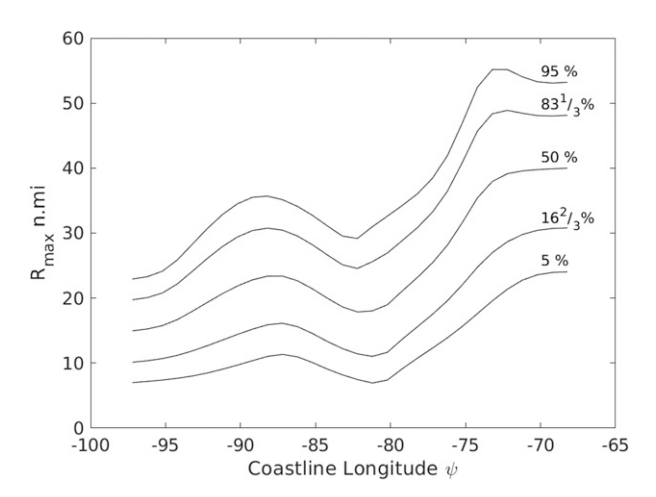


FIG. A2. Observed quantiles of $R_{\rm max}$ as a function of the U.S. coast-line longitude ψ reproduced from Figs. 37 and 38 of Ho et al. (1987) and compared with Fig. 7 of Casson and Coles (2000). The $R_{\rm max}$ increases as a function of the latitude as seen in the figure (increases and decreases along the U.S. coastline defined longitude). The model for $R_{\rm max}$ is created using the longitude ψ , whereas sampling is performed using the latitude ϕ because $R_{\rm max}$ is unique along ϕ .

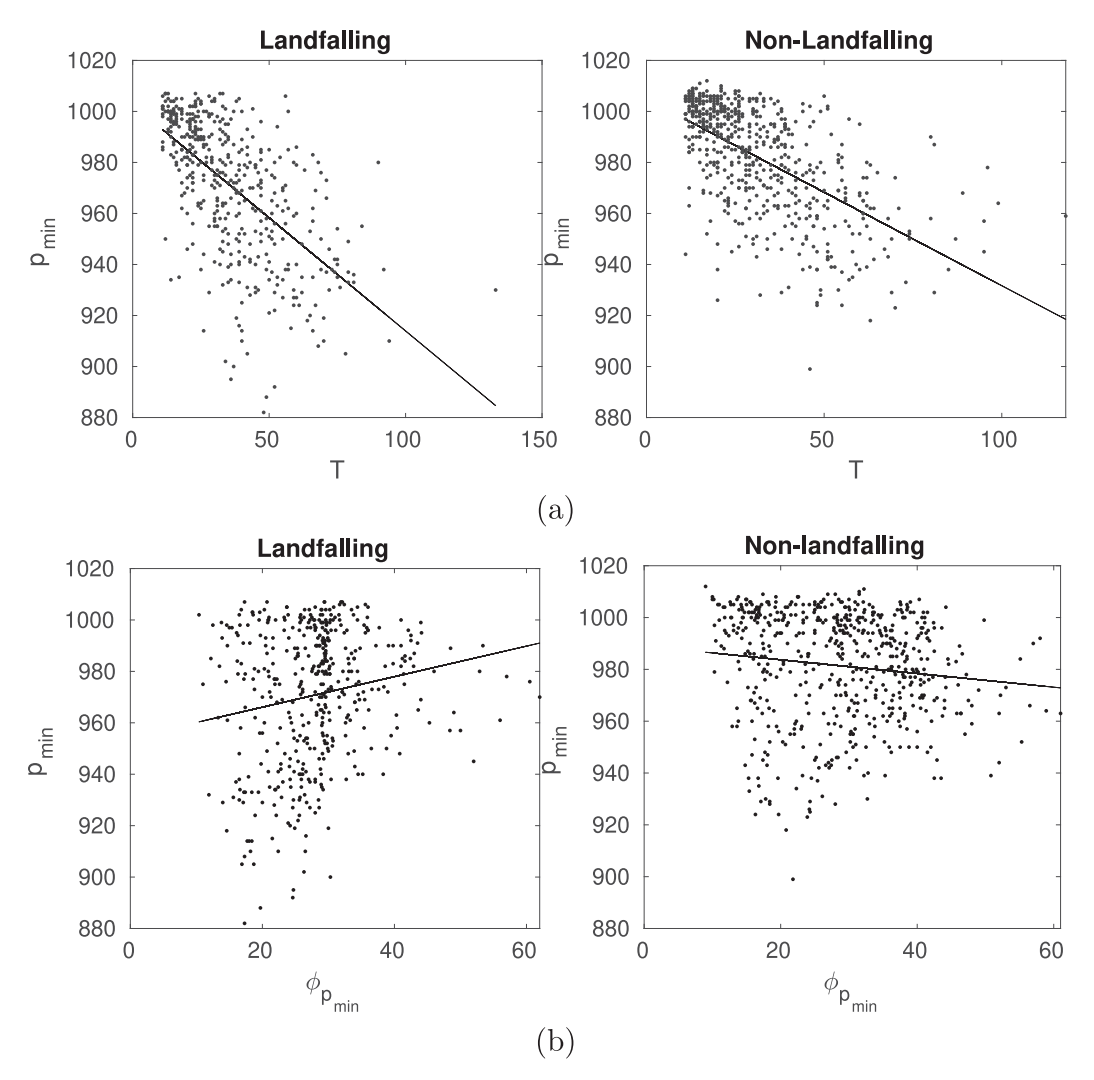


FIG. C1. Scatterplots of p_{\min} against (a) T and (b) $\phi_{I_{p_{\min}}}$ for (left) landfalling and (right) nonlandfalling hurricanes, with a line of best fit added.

- Simulate a hurricane track by uniformly sampling a historical track and adding a small amount of spatial noise at each step sampled from $\mathcal{N}(0, \sigma^2)$, where $\sigma \simeq 100$ n mi (~185 km).
- Uniformly sample a central pressure time series of a nonlandfalling hurricane.
- Time scale the central pressure time series to match the lifetime of the simulated track.
- For simulated landfalling hurricanes, run a Bernoulli trial with p probability that the time of occurrence of the central pressure minimum occurring is at landfall, $t_{p_{\min}} = t_{\text{lf}}$, and 1 p otherwise (p is estimated from the database).
- If occurring before landfall, randomly sample the time of occurrence for central pressure minimum using the density of the ratio t_{pmin}/t_{If} in Fig. A1.*
 Randomly sample the central pressure minimum
- Randomly sample the central pressure minimum from the nonstationary model described by Eqs. (5) and (6).*

- Randomly sample the central pressure range using the density model in Casson and Coles (2000, their section 2.5) with fits in Table A1.
- Add landfall effects described in Casson and Coles (2000, their section 2.6) separately for inland and coastal hurricanes.
- Simulate the radius to maximum wind speeds $R_{\text{max}}(\phi_t)$ by finding the distribution with coastal latitude ϕ_t illustrated in Fig. A2.
- Use the simulated central pressure time series p_t and $R_{\text{max}}(\phi_t)$ as inputs into the wind field model described in Eq. (1).

APPENDIX B

The Locally Stationary Model for Central Pressure Minima

The locally stationary model proposed by Casson and Coles (2000) is given by

$$\mu = \mu_0 + \mu_1 \log(T) + \mu_2 \phi_{t_{p_{\min}}}, \quad \sigma = \sigma_0, \quad k = k_0,$$
 (B1)

for landfalling hurricanes and

$$\mu = \mu_0 + \mu_1 \log(T), \quad \sigma = \sigma_0 + \sigma_1 \phi_{t_{p_{\min}}}, \quad k = k_0, \quad (B2)$$

for nonlandfalling hurricanes.

APPENDIX C

Additional Scatterplots

This appendix presents scatterplots (Fig. C1) of the central pressure minima against the lifetime T and latitude $\phi_{t_{p_{min}}}$ for landfalling and nonlandfalling hurricanes. The results indicate that the stationary model including dependence on T and $\phi_{t_{p_{min}}}$ is a reasonable starting point for forming the nonstationary model.

REFERENCES

- Batts, M. E., M. R. Cordes, L. R. Russell, and E. S. J. R. Shaver, 1980: Hurricane wind speeds in the United States. U.S. Department of Commerce National Bureau of Standards Doc., 60 pp., https://nvlpubs.nist.gov/nistpubs/Legacy/BSS/nbsbuildingscience124.pdf.
- Bloemendaal, N., I. Haigh, H. Moel, S. Muis, R. Haarsma, and J. Aerts, 2020: Generation of a global synthetic tropical cyclone hazard dataset using storm. Sci. Data, 7, 40, https://doi.org/10. 1038/s41597-020-0381-2.
- Carney, M., and H. Kantz, 2020: Robust regional clustering and modeling of nonstationary summer temperature extremes across Germany. Adv. Stat. Climatol. Meteor. Oceanogr., 6, 61–77, https://doi.org/10.5194/ascmo-6-61-2020.
- —, R. Azencott, and M. Nicol, 2019: Nonstationarity of summer temperature extremes in Texas. *Int. J. Climatol.*, 40, 620–640, https://doi.org/10.1002/joc.6212.
- Casson, E., and S. Coles, 2000: Simulation and extremal analysis of hurricane events. *Appl. Stat.*, 49, 227–245, https://doi.org/ 10.1111/1467-9876.00189.
- Coles, S., 2001: An Introduction to Statistical Modeling of Extreme Values. Springer, 219 pp.
- Cooley, D., 2013: Return periods and return levels under climate change. Extremes in a Changing Climate: Detection, Analysis and Uncertainty, A. AghaKouchak et al., Eds., Vol. 65, Springer, 97–114.
- Donaldson, T., 1966: Power of the *F*-test for nonnormal distributions and unequal error variances. RAND Corporation Tech. Rep., 66 pp.
- Hirsch, M., A. DeGaetano, and S. Colucci, 2001: An East Coast winter storm climatology. J. Climate, 14, 882–899, https://doi. org/10.1175/1520-0442(2001)014<0882:AECWSC>2.0.CO;2.
- Ho, F. P., J. C. Su, K. L. Smith, and F. P. Richards, 1987: Hurricane climatology for the Atlantic and Gulf Coasts of the United States. NOAA Tech. Rep. NWS 38, 195 pp., https://coast.noaa.gov/data/hes/images/pdf/ATL_GULF_HURR_CLIMATOLOGY.pdf.
- Hollander, M., D. Wolfe, and E. Chicken, 2015: Nonparametric Statistical Methods. 3rd ed. Wiley Series in Probability and Statistics, John Wiley and Sons, 819 pp.
- Keim, B., R. Muller, and G. Stone, 2004: Spatial and temporal variability of coastal storms in the North Atlantic basin. *Mar. Geol.*, 210, 7–15, https://doi.org/10.1016/j.margeo.2003.12.006.

- Kim, H., S. Kim, H. Shin, and J. H. Heo, 2017: Appropriate model selection for nonstationary generalized extreme value models. J. Hydrol., 547, 557–574, https://doi.org/10.1016/j. jhydrol.2017.02.005.
- Knight, K., 2002: What are the limiting distributions of quantile estimators? Statistics for Industry and Technology, Birkhäuser, 47–65.
- Knutson, T. R., and Coauthors, 2019: Tropical cyclones and climate change assessment: Part I: Detection and attribution. Bull. Amer. Meteor. Soc., 100, 1987–2007, https://doi.org/10.1175/BAMS-D-18-0189.1.
- Landsea, C. W., and J. L. Franklin, 2013: Atlantic hurricane database uncertainty and presentation of a new database format. *Mon. Wea. Rev.*, 141, 3576–3592, https://doi.org/10.1175/ MWR-D-12-00254.1.
- —, G. Vecchi, L. Bengtsson, and T. R. Knutson, 2010: Impact of duration thresholds on Atlantic tropical cyclone counts. *J. Cli*mate, 23, 2508–2519, https://doi.org/10.1175/2009JCL13034.1.
- Leadbetter, M. R., 1974: On extreme values in stationary sequences. Z. Wahrscheinlichkeitstheorie Verw. Geb., 28, 289–303.
- —, G. Lindgren, and H. Rootzén, 1983: Extremes and Related Properties of Random Sequences and Processes. Springer Series in Statistics, Springer Verlag, 336 pp.
- Lucarini, V., and Coauthors, 2016: Extremes and Recurrence in Dynamical Systems. Pure and Applied Mathematics, John Wiley and Sons, 312 pp.
- Muller, C., and Y. Takayabu, 2020: Response of precipitation extremes to warming: What have we learned from theory and idealized cloud-resolving simulations, and what remains to be learned. *Environ. Res. Lett.*, 15, 035001, https://doi.org/10.1088/1748-9326/ab7130.
- NOAA, 1972: Revised standard project hurricane criteria for the Atlantic and Gulf Coasts of the United States. NWS Memo. HUR 7-120, 47 pp.
- Patricola, C., and M. Wehner, 2018: Anthropogenic influences on major tropical cyclone events. *Nature*, **563**, 339–346, https://doi.org/10.1038/s41586-018-0673-2.
- Salas, J. D., and J. Obeysekera, 2014: Revisiting the concepts of return period and risk for nonstationary hydrologic extreme events. J. Hydrol. Eng., 19, 554–568, https://doi.org/10.1061/ (ASCE)HE.1943-5584.0000820.
- Simiu, E., N. A. Heckert, and T. Whalen, 1995: Estimates of hurricane wind speeds by the 'peaks over threshold' method. NIST Tech. Note 1416, 50 pp.
- Trepanier, J., 2020: North Atlantic hurricane winds in warmer than normal seas. *Atmosphere*, **11**, 293, https://doi.org/10.3390/atmos11030293.
- Vecchi, G. A., and T. R. Knutson, 2007: On estimates of historical North Atlantic tropical cyclone activity. J. Climate, 21, 3580– 3600, https://doi.org/10.1175/2008JCLI2178.1.
- —, and —, 2010: Estimating annual numbers of Atlantic hurricanes missing from the HURDAT database (1878–1965). *J. Climate*, 1738–1745, https://doi.org/10.1175/2010JCLI3810.1.
- —, C. W. Landsea, W. Zhang, G. Villarini, and T. R. Knutson, 2021: Changes in Atlantic major hurricane frequency since the late-19th century. *Nat. Commun.*, **12**, 4054, https://doi.org/ 10.1038/s41467-021-24268-5.
- Vickery, P. J., and L. A. Twisdale, 1995: Prediction of hurricane wind speeds in the US. *J. Struct. Eng.*, **121**, 1691–1699, https://doi.org/10.1061/(ASCE)0733-9445(1995)121:11(1691).
- Yamaguchi, M., J. C. L. Chan, I.-J. Moon, K. Yoshida, and R. Mizutas, 2020: Global warming changes tropical cyclone translation speed. *Nat. Commun.*, 11, 47, https://doi.org/10.1038/s41467-019-13902-y.